

Very Massive Stars: Near and Far

Sébastien Martinet¹ , Georges Meynet¹, Sylvia Ekström¹,
Cyril Georgy¹, Lionel Haemmerlé¹, Devesh Nandal¹ 
and Raphael Hirschi^{2,3}

¹Geneva Observatory, University of Geneva, Chemin Pegasi 51, CH-1290 Versoix, Switzerland
email: sebastien.martinet@unige.ch

²Astrophysics Group, Keele University, Keele, Staffordshire, ST5 5BG, UK

³Institute for Physics and Mathematics of the Universe (WPI), University of Tokyo, 5-1-5
Kashiwanoha, Kashiwa 277-8583, Japan

Abstract. In addition to being spectacular objects, very massive stars (VMS) are suspected to have a tremendous impact on their environment and on the whole cosmic evolution. The nucleosynthesis both during their advanced stages and their final explosion likely contribute greatly to the overall enrichment of the Universe. Their resulting Supernovae are candidates for the most superluminous events and their extreme conditions lead also to very important radiative and mechanical feedback effects, from local to cosmic scale. With the recent implementation of a new equation of state in the GENEC stellar evolution code, appropriate for describing the conditions in the central regions of very massive stars in the advanced phases, we present new results on VMS evolution from Population III to solar metallicity. We explore their evolution and final fate as potential (P)PISNe across the cosmic time. We compare our results to recent spectroscopic observations of VMS in the Large Magellanic Cloud (LMC). We also underline the important radiative feedback of Population III VMS during the reionization epoch and the chemical contribution of these stars at high metallicity, especially for short-lived radionuclei.

Keywords. stars: evolution, stars: supernovae, stars: fundamental parameters

1. Introduction

The Tarantula Nebula in the Large Magellanic Cloud hosts one particular young cluster, known as R136, hosting itself very high mass components. A first spectroscopic study by Cassinelli et al. (1981) showed the presence of very strong P-Cygni features for the center object of this cluster, characteristic of very high ionization flux. From this measurement, they obtained that the central object must either be a few thousands solar masses, or an unresolved cluster of stars. The latter was the solution, found with the observations of Crowther et al. (2006), first with stars ranging up to $150M_{\odot}$, and then up to $300M_{\odot}$ after further studies (Crowther et al. 2010). Recent work (Bestenlehner et al. 2020; Brands et al. 2022) confirmed these results with new VLT-FLAMES and HST/STIS optic/spectroscopic measurements and provide interesting stellar characteristics to the most massive stars observed. With the new VMS models computed here, we can confront our results to these new observations and explore the impact of the different physics included.

2. Methods

We present a new grid of VMS models, with initial masses of 180, 250 and $300M_{\odot}$, including the new EOS for high temperature/density regimes, probing $Z=0.000$, $Z=10^{-5}$,

$Z=0.006$ and $Z=0.014$ metallicities for non-rotating and rotating models at $V/V_c=0.4$ where V_c is the critical velocity. We adopt an overshooting value of $\alpha_{ov}=0.2$ following the results of [Martinet et al. \(2021\)](#). We used the Ledoux criterion to determine the position of the convective boundaries, as there are some indications that the Ledoux criterion might be more appropriate ([Georgy et al. 2014](#); [Kaiser et al. 2020](#)) for these VMS. The radiative mass-loss rate adopted on the MS is from [Vink et al. \(2001\)](#); the domains not covered by this prescription (see Fig. 1 of [Eggenberger et al. 2021](#)) use the [de Jager et al. \(1988\)](#) rates. [Gräfenor & Hamann \(2008\)](#) prescriptions are used in their domain of application, while [Nugis & Lamers \(2000\)](#) prescriptions are used everywhere else for the Wolf-Rayet phase[†]. The radiative mass-loss rate correction factor described in [Maeder & Meynet \(2000\)](#) is applied for rotating models. The dependence on metallicity is taken such that $\dot{M}(Z) = (Z/Z_\odot)^{0.7} \dot{M}(Z)$, except during the red supergiant (RSG) phase, for which no dependence on the metallicity is used. This is done accordingly to [van Loon et al. \(2005\)](#) and [Groenewegen \(2012a,b\)](#) showing that the metallicity dependence for the mass loss rates of these stars do appear to be weak. For the rotation prescription, the models use the shear diffusion coefficient as given by [Maeder \(1997\)](#) and the horizontal diffusion coefficient from [Zahn \(1992\)](#).

3. Comparison with observed VMS in the LMC

Fig. 1 presents the HRD of the Tarantula Nebula, a very active region in the LMC. The compilation of [Schneider et al. \(2018\)](#) is displayed in yellow, while the components of the R136 cluster, obtained by [Brands et al. \(2022\)](#), are displayed in magenta. The tracks used here are the $Z=0.006$ GENE tracks from [Eggenberger et al. \(2021\)](#) and the VMS tracks we computed for this work with the new EOS. We can see that this cluster hosts several high-mass components. If we look at the evolution of our VMS models, three stars inside this cluster are above $M_{ini}=200M_\odot$. If we start with the HRD tracks, we can wonder if either the non-rotating or the rotating models fit better their position in the HRD. At first glance, one would favor the non-rotating models, covering a large range of effective temperature on the MS, while the rotating models evolve quasi-chemically homogeneously and stray directly to the bluer part of the HRD, hence incompatible with the observed effective temperature. The picture is however not that easy, as we have indeed seen, the VMS at high metallicity undergo very large mass loss already during the MS. This means, in fact, that the star is embedded inside a “nebula” of very thick wind. When observing such stars, we observe in fact this thick wind, and this blurs the determination of the effective temperature of the surface of the star. Indeed, the wind being much cooler than the surface of the star, we would obtain a lower effective temperature to be observed if we took this effect into account. In fact, if we correct for this process, both non-rotating and rotating models are compatible with the observations.

The evolution of VMS at high metallicity is dominated by mass loss. The prescriptions used in our models are empirical results obtained from lower mass O-type stars, and are a highly controversial topic recently, with new mass loss rates proposed to be both much lower than previously used, or the other way round, much higher, in particularly when getting close to the Eddington limit (see the review of [Vink 2021](#)). We confront in Fig. 2 our models to the observed mass loss rates obtained by [Brands et al. \(2022\)](#) and their corresponding fit using the prescription proposed by [Bestenlehner et al. \(2020\)](#). The mass loss rates are plotted as a function of the Eddington parameter (with $\Gamma_{edd,e}=1$ being the Eddington limit). Interestingly, the mass loss we obtain on the MS from the prescriptions

[†] The Wolf-Rayet phase in GENE is assumed to begin when the model has an effective temperature larger than 10 000 K and a surface mass fraction of hydrogen at the surface below 0.3.

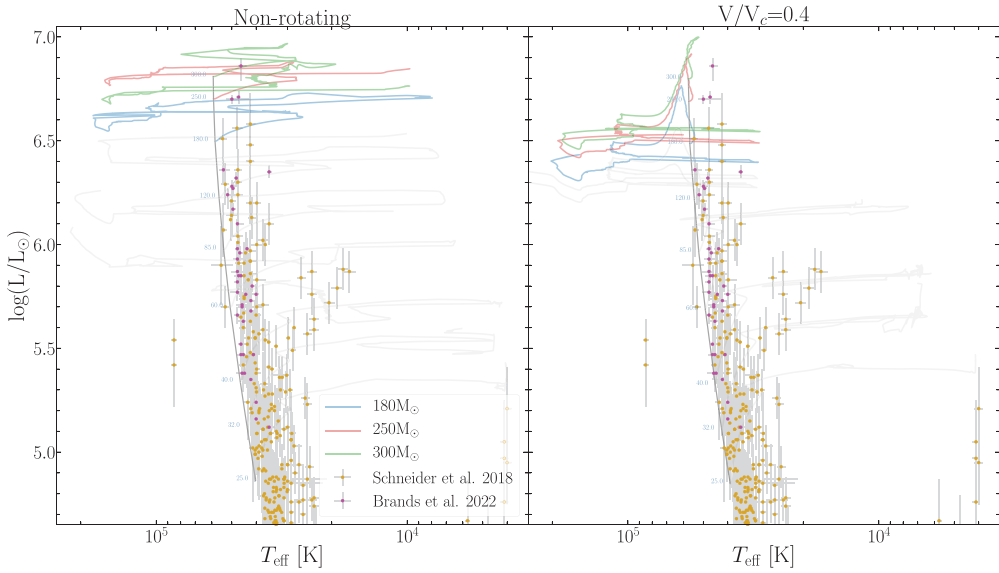


Figure 1. HRD of the Tarantula Nebula from the compilation of Schneider et al. (2018) (regrouping results from Ramírez-Agudelo et al. 2017; Sabín-Sanjulián et al. 2014, 2017; McEvoy et al. 2015; Bestenlehner et al. 2014) and the R136 cluster members from the work of Brands et al. (2022). The GENEC tracks are overplotted in grey, with color emphasis on the VMS models computed here, and the ZAMS is drawn in dark grey. The HRD is plotted for non-rotating (left) and rotating at $V/V_c=0.4$ (right) models.

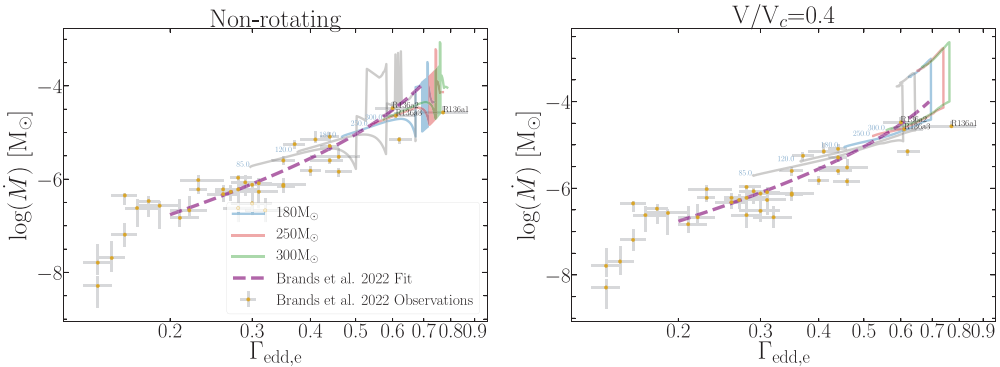


Figure 2. Mass loss rates as a function of the Eddington parameter $\Gamma_{\text{edd},e}$. The tracks of 85–120 M_{\odot} are from Eggenberger et al. (2021), and the 180–300 M_{\odot} from this work. The observations of Brands et al. (2022) of the R136 components are displayed in gold. The fit they obtained is displayed in purple.

we use are actually in quite good agreement with the observations for the most massive models, and for both the non-rotating and the rotating ones.

As we have spectroscopic observations of these stars, we can obtain surface velocities for the VMS observed in this cluster. The left panel of Fig. 3 shows the values obtained by Bestenlehner et al. (2020) overplotted over the tracks of VMS models. From the spectroscopic studies, the surface velocities observed do not differentiate the surface velocity from the macro-turbulent velocity. This means that the lower limit of the surface velocity would be when the macro-turbulent is at a maximum. We take the maximum macro-turbulent velocities obtained by Simón-Díaz et al. (2017) for stars close to the Eddington limit to obtain the lower uncertainties displayed. The upper limit is obtained from the

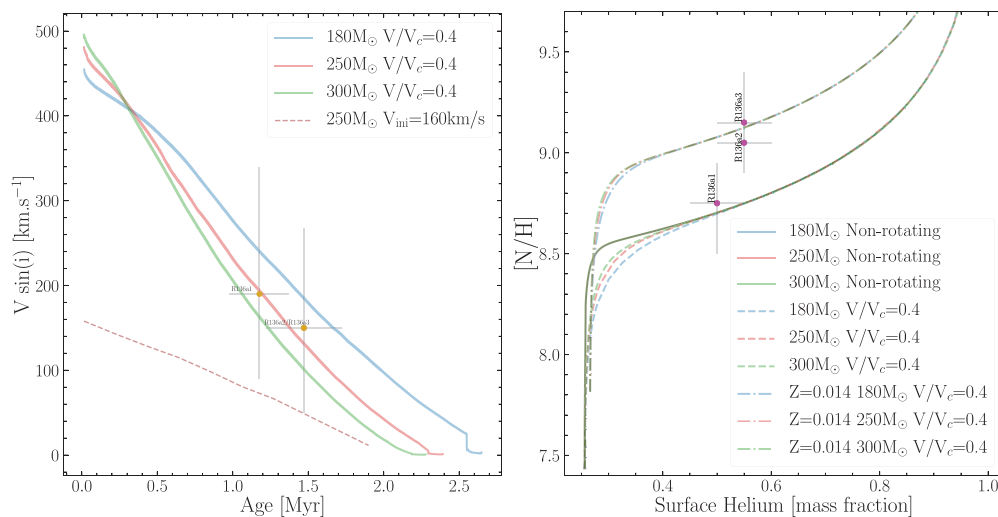


Figure 3. *Left:* Evolution of the surface velocity of VMS models. An additional model with slower initial rotation rate has been computed for this plot. The observed velocities of the three most massive components of R136 have been overplotted (R136a2 and R136a3 have similar velocity obtained). *Right:* Surface enrichment of Nitrogen over Hydrogen as a function of the surface Helium. The observed values of $[N/H]$ are from Brands *et al.* (2022), and the surface Helium fraction from Bestenlehner *et al.* (2020).

angle of view effects. We see that the surface velocity is quickly decreasing during the MS due to the large mass loss taking away angular momentum from the envelope, combined to the differential rotation. To obtain the values of the surface velocities observed by Bestenlehner *et al.* (2020) at this stage of the MS, we need quite high rotation rates already at the ZAMS from the physics we included in these models. Indeed, we computed a $250M_{\odot}$ model with lower rotation rate to show that the mass loss still dominates the surface velocity evolution and would not be able to reproduce the high velocities observed for these VMS. To reproduce such high values of surface velocity with lower initial rotation rate, it would be needed to have stronger angular momentum transport inside the star (such as internal magnetic fields) to counteract the large decrease from the mass loss.

The right panel of Fig. 3 shows the observed surface enrichment of Nitrogen as a function of the observed surface Helium respectively from Brands *et al.* (2022) and Bestenlehner *et al.* (2020). The non-rotating (in plain lines) and the rotating (in dashed lines) VMS models are overplotted. Interestingly, the evolution of Nitrogen at the surface is very similar between the non-rotating and rotating models. This is because the models quickly reach (before the surface Helium fraction reaches 0.4) the maximum quantity of Nitrogen produced from the CNO cycle in these stars. This quantity depends solely on the initial abundances of CNO. Hence, while the most massive component R136a1 is well reproduced by the models, there is no possibility for these models to explain the very high enrichment value of Nitrogen at this fraction of Helium at the surface of the two other VMS (R136a2/a3). Understanding these discrepancies is difficult, with multiple sources from which they could originate. First, the initial abundances and mixture of CNO could be different from the one used in these $Z=0.006$ models, leading to not enough nitrogen being able to be produced and brought to the surface. We can see that the $Z=0.014$ models are able to reproduce such value due to the larger initial abundances of CNO. Second, observational uncertainties cannot be ruled out. Indeed, even if the uncertainties are quantified in these studies, it is not excluded that both unexpected observational and

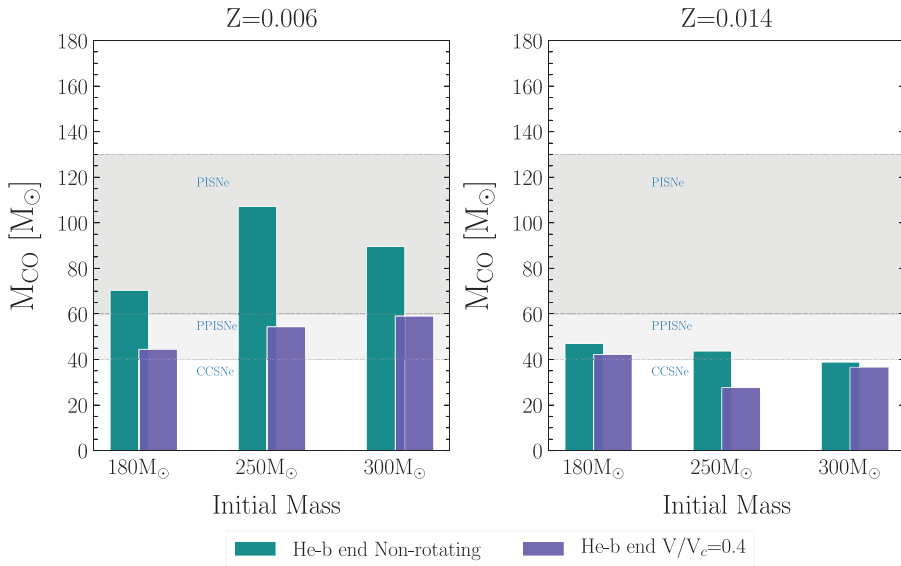


Figure 4. Evolution of the CO core mass of VMS stars at the end of the He-burning phase, for non-rotating and $V/V_c=0.4$ models at both $Z=0.006$ and $Z=0.014$. The(P)PISNe regions are from Farmer et al. (2019).

interpretational effects are present. Third, we can wonder of course if past history of the star, such as binary interaction or early merger could have such effect. A mass transfer from close binary interaction would explain a decrease of the surface Helium by bringing fresh Hydrogen, but would also diminish the $[N/H]$ ratio, and hence cannot explain the nitrogen surface enrichment. An early merger, on the other hand, would simply have at most the maximum quantity from the addition of the initial CNO abundances of both stars, and hence would still leave us with the same problem.

Fig. 4 shows the evolution of the CO core mass of VMS at the end of the He-burning phase, for different rotation rates and metallicities. At the beginning of He-burning, the mass of the core is dominated by the initial mass for the models at $Z=0.006$ while the stronger line-driven winds occurring for $Z=0.014$ models result in a large diminution of the core masses, becoming stronger for higher initial masses. During the He-burning phase, the WR winds drive the diminution of the core mass. However, due to their evolution, non-rotating models are undergoing additional mass losses due to their proximity to the Eddington limit. This results for the core masses of models at $Z=0.006$ to peak at 250 M_{\odot} and then to diminish for higher initial masses. For non-rotating models at $Z=0.014$, it results to obtain fairly similar core masses at the end of the He-burning phase. All in all, it means that the final fate of this VMS at high metallicity is extremely dependent on both the mass loss rates and the potential extra mixing from rotation. The combination outcome of the two is not trivial, as the resulting evolution can also drive additional mass loss. The final fate can be then extremely different between non-rotating and rotating stars.

4. Conclusions

Very massive stars, while very rare, are extreme objects that can have a very large chemical, mechanical and radiative feedback on a whole stellar population. Indeed, their extreme evolution, combined to very large mass losses could make them important contributors to nucleosynthesis, especially for short-lived radionuclides (see Martinet et al.

2022). Moreover, Population III VMS produce large quantities of ionizing photons, and could make them very important contributors during the reionization epoch (Murphy *et al.* 2021). We now observe such VMS in the LMC, confirming the large mass loss rates predicted by the models, and their strong ionization flux. These VMS need high initial rotation rates according to our models to explain their current fast rotation on the MS. However, surface enrichment is not well understood, and could be the result of either different initial composition than expected or from past interactions. More in-depth studies of the mass loss rates effects on these VMS is crucial (Higgins *et al.* 2021; Vink 2021) to understand their observed features.

References

- Bestenlehner, J. M., *et al.* 2014, *A&A*, 570, A38
 —. 2020, *MNRAS*, 499, 1918
 Brands, S. A., *et al.* 2022, arXiv e-prints, arXiv:2202.11080
 Cassinelli, J. P., Mathis, J. S., & Savage, B. D. 1981, *Science*, 212, 1497
 Crowther, P. A., Lennon, D. J., & Walborn, N. R. 2006, *A&A*, 446, 279
 Crowther, P. A., Schnurr, O., Hirschi, R., Yusof, N., Parker, R. J., Goodwin, S. P., & Kassim, H. A. 2010, *MNRAS*, 408, 731
 de Jager, C., Nieuwenhuijzen, H., & van der Hucht, K. A. 1988, *A&AS*, 72, 259
 Eggenberger, P., *et al.* 2021, *A&A*, 652, A137
 Farmer, R., Renzo, M., de Mink, S. E., Marchant, P., & Justham, S. 2019, *ApJ*, 887, 53
 Georgy, C., Saio, H., & Meynet, G. 2014, *MNRAS*, 439, L6
 Gräfener, G., & Hamann, W. R. 2008, *A&A*, 482, 945
 Groenewegen, M. A. T. 2012a, *A&A*, 540, A32
 —. 2012b, *A&A*, 541, C3
 Higgins, E. R., Sander, A. A. C., Vink, J. S., & Hirschi, R. 2021, *MNRAS*, 505, 4874
 Kaiser, E. A., Hirschi, R., Arnett, W. D., Georgy, C., Scott, L. J. A., & Cristini, A. 2020, *MNRAS*
 Maeder, A. 1997, *A&A*, 321, 134
 Maeder, A., & Meynet, G. 2000, *A&A*, 361, 159
 Martinet, S., *et al.* 2021, *A&A*, 648, A126
 —. 2022, arXiv e-prints, arXiv:2205.15184
 McEvoy, C. M., *et al.* 2015, *A&A*, 575, A70
 Murphy, L. J., Groh, J. H., Farrell, E., Meynet, G., Ekström, S., Tsiatsiou, S., Hackett, A., & Martinet, S. 2021, *MNRAS*
 Nugis, T., & Lamers, H. J. G. L. M. 2000, *A&A*, 360, 227
 Ramírez-Agudelo, O. H., *et al.* 2017, *A&A*, 600, A81
 Sabín-Sanjulián, C., *et al.* 2014, *A&A*, 564, A39
 —. 2017, *A&A*, 601, A79
 Schneider, F. R. N., *et al.* 2018, *A&A*, 618, A73
 Simón-Díaz, S., Godart, M., Castro, N., Herrero, A., Aerts, C., Puls, J., Telting, J., & Grassitelli, L. 2017, *A&A*, 597, A22
 van Loon, J. T., Cioni, M. R. L., Zijlstra, A. A., & Loup, C. 2005, *A&A*, 438, 273
 Vink, J. S. 2021, arXiv e-prints, arXiv:2109.08164
 Vink, J. S., de Koter, A., & Lamers, H. J. G. L. M. 2001, *A&A*, 369, 574
 Zahn, J.-P. 1992, *A&A*, 265, 115

Discussion

QUESTION: Is there observable allowing us to disentangle between PISNe coming from non-rotating progenitors and from rotating ones ?

MARTINET S.: While we still did not observe any confirmed PISN, we can see from Fig. 4 that rotation can have very different effects at different metallicities, due to the

different evolution pathways. Indeed, a rotating model is usually expected to increase the size of the core through rotational mixing. However, the extra mixing also bring the star to evolve in a quasi-chemically homegenous way, reaching much faster the WR phase. This triggers large mass loss that do not occur as early in non-rotating models. In fact, it results in final CO core masses much smaller for rotating models than for non-rotating ones.